Inorg. Chem. **2008**, *47*, 9941−9945

Crystal Growth of Two New Photoluminescent Oxides: $Sr_3Li_6Nb_2O_{11}$ and $Sr_3Li_6Ta_2O_{11}$

M. Bharathy, V. A. Rassolov, S. Park, and H.-C. zur Loye*

Department of Chemistry and Biochemistry, University of South Carolina, Columbia, South Carolina 29208

Received June 16, 2008

Single crystals of $Sr_3Li_6M_2O_{11}$ (M = Nb, Ta) were grown out of a high-temperature $Sr(OH)_2$/LiOH/KOH flux. The single crystal X-ray diffraction data were indexed to the orthorhombic *Pmma* system, with a = 10.5834(15) Å, b = 8.3103(13) Å, c = 5.8277(8) Å, V = 512.55(13) Å^3, and Z = 2 for $Sr_3Li_6Nb_2O_{11}$ and a = 10.5936(6) Å, b = 8.3452(5) Å, c = 5.8271(4) Å, V = 515.15(6) Å^3, and Z = 2 for $Sr_3Li_6Ta_2O_{11}$. The crystal structure consists of sheets of interconnected SrO_8 polyhedra that are separated by M−O layers and an intervening LiO_x polyhedral framework, representing a new structural type. The M−O layers exhibit a rare occurrence of both five- and six-coordinated M^{5+} ions in the same structure. The oxides, upon excitation at 250 nm, exhibit violet emission at room temperature.

Introduction

Niobates and tantalates in the $AO-A_2'O-M_2O_5$[1−20] system (A = Ca^{2+}, Sr^{2+}, Ba^{2+}; A' = Li^+, Na^+, Rb^+; M = Nb^{5+}/Nb^{4+}, Ta^{5+}/Ta^{4+}) commonly crystallize in the perovskite or perovskite-related structure types, including $Ca_2A'M_3O_{10}$ (A' = Li^+, Na^+, K^+, Rb^+, Cs^+, NH_4^+, Tl^+; M = Nb^{5+}, Ta^{5+}),[1−3] $Ca_2A'_2Ta_3O_{10}$[4] (A' = Li, Na), $Li_{2x}Ca_{0.5-x}TaO_3$,[5] $Li_{0.2}(Ca_{1-y}Sr_y)_{0.4}TaO_3$,[5] $Ca_4NaNb_5O_{17}$,[6,7] $Ca_2Na_2Nb_4O_{13}$,[8,9] $Sr_xNa_{1-x}NbO_3$,[10] $Ba_4LiM_3O_{12}$,[11−13] and A_3NaMO_6 (M = Nb, Ta),[19,20] as well as in less commonly observed structure types including Ruddlesden−Popper-related compounds ($Li_4Sr_3Nb_6O_{20}$,[14] $Li_2SrNb_2O_7$[17]), anion-deficient pyrochlores ($SrNaNb_2O_{6.5}$),[15] rock salt structures ($Ca_2Na_3TaO_6$),[16] and tetragonal tungsten bronzes ($Ba_2NaNb_5O_{15}$).[18] In almost all cases, polycrystalline samples of these oxides were synthesized by the traditional solid-state or ion-exchange methods,[1,2,15] while single crystals were obtained from sulfate and carbonate fluxes.[8] For the syntheses of alkali and alkaline-earth metal substituted niobates and tantalates, the solid-state method requires high sintering temperatures owing to the low reactivities of the starting transition metal oxides, Nb_2O_5 and Ta_2O_5. The preferential loss of the alkali metal oxides (Na_2O, Li_2O) at high temperatures can be a problem in the solid-state approach, as well as during crystal growth from high-temperature solutions. To minimize this issue, one alternative synthetic route has been the use of low-temperature fluxes as solvents for crystal growth, where it is known that hydroxide fluxes are an effective low-temperature solvent. By contrast, other effective solvents, such as sulfate and carbonate fluxes, require significantly higher temperatures.

Over the past decade, it has been repeatedly demonstrated that hydroxide fluxes constitute an excellent solvent media at relatively low temperatures (500−700 °C) for the crystal growth of a multitude of alkali−alkaline earth metal substituted oxides containing transition metals such as V^{5+}, Nb^{5+}, Ta^{5+}, Ru^{5+}, and Os^{7+}.[20−25] In this article, we report the crystal growth of pale green, centimeter-sized crystals

* Author to whom correspondence should be addressed. Phone: +1-803-777-6916. Fax: +1-803-777-8508. E-mail: zurloye@mail.chem.sc.edu.

(1) Dion, M.; Ganne, M.; Tournoux, M. *Mater. Res. Bull.* **1981**, *69*, 1429.
(2) Toda, K.; Sato, M. *J. Mater. Chem.* **1996**, *6*, 1067.
(3) Byeon, S.-H.; Jin, K. H.; Kim, D.-K.; Hwi, H. N *Chem. Mater.* **2003**, *15*, 383.
(4) Toda, K.; Takahashi, M.; Teranishi, T.; Ye, Z.-G.; Sato, M.; Hinatsu, Y. *J. Mater Chem.* **1999**, *9*, 799.
(5) Nghi, P. Q.; Crosnier-Lopez, M. P.; Le Berre, F.; Fauth, F.; Fourquet, J.-L. *Solid State Sci.* **2004**, *6*, 923.
(6) Zuniga, F. J.; Darriet, J. *Acta Crystallogr.* **2003**, *C59*, 18.
(7) Elcoro, L.; Zuniga, F. J.; Perez-Mato, J. M. *Acta Crystallogr.* **2004**, *B60*, 21.
(8) Chiba, K.; Ishizawa, N.; Nagai, Y.; Oishi, S. *Solid State Ionics.* **1998**, *108*, 179.
(9) Chiba, K; Ishizawa, N; Oishi, S. *Acta Crystallogr.* **1999**, *55*, 1041.
(10) Istomin, S. Ya.; Svensson, G.; Koehler, J. *J. Solid State Chem.* **2002**, *167*, 7.
(11) Negas, T.; Roth, R. S.; Parker, S.; Brower, W. S. J. *Solid State Chem.* **1973**, *8*, 1.
(12) Jendrek, E. F.; Potoff, A. D.; Katz, L. *J. Solid State Chem.* **1974**, *9*, 375.
(13) Jendre Collins, B. M.; Jacobson, A. J.; Fender, B. E. F. *J. Solid State Chem.* **1974**, *10*, 29.

10.1021/ic801102t CCC: $40.75
Published on Web 10/10/2008

Table 1. Crystallographic Data of $Sr_3Li_6Nb_2O_{11}$ and $Sr_3Li_6Ta_2O_{11}$

empirical formula	$Sr_3Li_6Nb_2O_{11}$	$Sr_3Li_6Ta_2O_{11}$
cryst habit, color	block, pale green	block, pale green
cryst size (mm)	0.2 ×0.15 ×0.1	0.26 ×0.20 ×0.17
cryst syst	orthorhombic	orthorhombic
space group	*Pmma*	*Pmma*
cell dimensions (Å/°):	10.5834 (15)	10.5936 (6)
b	8.3103 (13)	8.3452 (5)
c	5.8277 (8)	5.8271(4)
volume (Å^3)	512.55(13)	515.15 (6)
formula weight	666.32	842.40
D_x (g/cm^3)	4.318	5.431
Z	2	2
F(000)	604	732
scan mode	ω scan	ω scan
θ_{max}	35.79	35.96
recording reciprocal space	$-17 \le h \le 17, -11 \le k \le 13, -3 \le l \le 9$	$-17 \le h \le 15, -13 \le k \le 8, -9 \le l \le 8$
number of measured reflns	4953	5227
number of independent reflns	1273 with $I > 3\sigma(I)$[R(int)=0.078]	1339 with $I > 3\sigma(I)$[R(int)=0.0823]
μ (mm^{-1})	17.228	36.638
refinement	F^2	F^2
no. of variables	66	66
$R(F)$	0.0396	0.049
$wR(F^2)$	0.1174	0.1158
GoF	1.569	1.134
Max/min $\Delta\rho$ e/Å^3	2.612/−1.221	2.031/−3.382

of $Sr_3Li_6M_2O_{11}$ (M = Nb, Ta) out of a hydroxide flux. Interestingly, these two oxides that crystallize in a new structure type, upon excitation at a wavelength of 250 nm, exhibit violet emission at room temperature. The crystal growth, structure, optical properties, and theoretical investigations on the possible mechanism of photoluminescence of $Sr_3Li_6M_2O_{11}$ (M = Nb, Ta) are reported herein.

Experimental Section

Materials. Nb_2O_5 (Alfa Aesar, 99.5%), Ta_2O_5 (Acros Organics, 99.5%), $Sr(OH)_2$ (Aldrich, 96%), KOH (Mallinckrodt Chemicals, reagent-grade), and $LiOH \cdot H_2O$ (Alfa Aesar, Reagent grade) were used as received.

Crystal Growth. Pale green, single crystals of $Sr_3Li_6Nb_2O_{11}$ and $Sr_3Li_6Ta_2O_{11}$ were grown from a $Sr(OH)_2$/LiOH/KOH flux contained in a silver crucible. Nb_2O_5 (0.2658 g, 1mmol), Ta_2O_5 (0.4418 g, 1mmol), $Sr(OH)_2$ (0.75 g, 6.1 mmol), $LiOH \cdot H_2O$ (6 g, 142.9 mmol), and KOH (3 g, 53.4 mmol) were placed into silver crucibles and covered loosely with silver lids. The crucibles were held at 600 °C (700 °C for $Sr_3Li_6Ta_2O_{11}$) for 12 h and slowly cooled to 500 °C (600 °C for $Sr_3Li_6Ta_2O_{11}$) over 1 h for $Sr_3Li_6Nb_2O_{11}$, after which time the furnace was turned off and the crucibles were allowed to cool to room temperature. The crystals were separated from the flux by dissolving the flux in methanol and subsequently isolated by vacuum filtration.

Single Crystal X-Ray Diffraction. Single crystal X-ray diffraction intensity data for $Sr_3Li_6M_2O_{11}$ ($M = Nb^{5+}$, Ta^{5+}) were collected on a Bruker SMART APEX CCD based diffractometer using monochromated Mo Kα radiation. Four sets of runs with ϕ angles of 0°, 90°, 180°, and 0° of 0.3° in frame width were collected to obtain a complete sphere in reciprocal space. Data were integrated using SAINTPLUS[26] in the SMART software suite. An empirical absorption correction was applied. Direct methods in the SHELXS97[27] software were employed to obtain the atomic positions of the niobium, tantalum, and strontium atoms. The oxygen and lithium atoms were located by subsequent difference Fourier syntheses. Sr, Nb, Ta, O, and Li atoms were refined with anisotropic displacement parameters using SHELXL97.[28] All of the atoms occupy special positions except O1 ($Sr_3Li_6Nb_2O_{11}$) and O5 ($Sr_3Li_6Ta_2O_{11}$). The lithium atoms are fully occupied at their crystallographic sites. Crystallographic data and details of the single crystal data collection of the $Sr_3Li_6M_2O_{11}$ ($M = Nb^{5+}$, Ta^{5+}) are listed in Table 1, and bond lengths and angles are listed in Table 2.

^{7}Li NMR Spectroscopy. ^{7}Li NMR spectra (194.4 MHz) were recorded on ground samples of $Sr_3Li_6M_2O_{11}$ ($M = Nb^{5+}$, Ta^{5+}) on a Varian Inova 500 NMR spectrometer equipped with a Doty XC/4 mm magic angle spinning probe. The samples were spun at 10 kHz, and Bloch decays were collected after 90° pulses. A relaxation delay of 3 s was used, and typically 4−8 transients were sufficient for adequate sensitivity. LiCl was used as an external chemical shift reference.

Optical Properties. The UV−visible diffuse reflectance spectra of crushed single crystals of $Sr_3Li_6M_2O_{11}$ ($M = Nb^{5+}$, Ta^{5+}) were obtained on a Shimadzu UV/vis NIR Scanning Spectrophotometer equipped with an integration sphere. The diffuse reflectance spectra were converted to absorbance spectra by the Kubelka−Munk

(14) Bhuvanesh, N. S. P.; Crosnier-Lopez, M. P.; Bohnke, O.; Emery, J.; Fourquet, J. L. *Chem. Mater.* **1999**, *11*, 634.
(15) Kim, J.-Y.; Chung, I.; Kim, S.-J.; Choy, J.-H. *J. Mater. Chem.* **2002**, *12*, 1001.
(16) Yamane, H.; Takahashi, H.; Kajiwara, T.; Shimada, M. *Acta Crystallogr.* **2000**, *C56*, 1177.
(17) Floros, N.; Michel, C.; Hervieu, M.; Raveau, B. *J. Mater Chem.* **1999**, *9*, 3101.
(18) Foulon, G.; Ferriol, M.; Brenier, A.; Boulon, G.; Lecocq, S. *Eur. J. Solid State Inorg. Chem* **1996**, *33*, 673.
(19) Wehrum, G.; Hoppe, R. *Z. Anorg. Allg. Chem.* **1992**, *617*, 45.
(20) Bharathy, M.; Rassolov, V.; zur Loye, H.-C. *Chem. Mater.* **2008**, *20*, 2268.
(21) Mugavero, S. J., III; Bharathy, M.; Alum., J. M.; zurLoye, H.-C. *Solid State Sci.* **2008**, *10*, 370.
(22) Davis, M. J.; Smith, M. D.; Stitzer, K. E.; zur Loye, H.-C. *J. Alloys Compd.* **2003**, *351*, 95.
(23) Stitzer, K. E.; Gemmill, W. R.; Smith, M. D.; zur Loye, H.-C. *J. Solid State Chem.* **2003**, *175*, 39.
(24) Stitzer, K. E.; Smith, M. D.; zur Loye, H.-C. *Solid State Ionics* **2002**, *4*, 211.
(25) Stitzer, K. E.; Abed, A. E.; Smith, M. D.; Davis, M.-J.; Kim, S. J.; Darriet, J.; zur.Loye, H.-C. *Inorg. Chem.* **2003**, *42*, 947.
(26) *SAINT*, version 6.45a; Bruker AXS Inc.: Madison, WI, 2000.
(27) Sheldrick, G. M. *SHELXS97*; University of Gottingen: Gottingen, Germany, 1997.
(28) Sheldrick, G. M. *SHELXL97*; University of Gottingen: Gottingen, Germany, 1997.

Table 2. Bond Lengths and Bond Valence Sums of $Sr_3Li_6Nb_2O_{11}$ and $Sr_3Li_6Ta_2O_{11}$

$Sr_3Li_6Nb_2O_{11}$		$Sr_3Li_6Ta_2O_{11}$	
Sr(1)−O(3) × 2	2.474(4)	Sr(1)−O(1) × 2	2.744(6)
Sr(1)−O(3) × 4	2.529(3)	Sr(1)−O(4) × 2	2.457(6)
Sr(1)−O(4) × 2	2.742(4)	Sr(1)−O(5) × 4	2.540(4)
bond valence sum	2.43	bond valence sum	
Sr(2)−O(4) × 2	2.544(2)	Sr(2)−O(3) × 2	2.536(3)
Sr(2)−O(1) × 2	2.553(3)	Sr(2)−O(5) × 2	2.556(4)
Sr(2)−O(2) × 2	2.6998(9)	Sr(2)−O(1) × 2	2.7011(9)
Sr(2)−O(3) × 2	2.749(2)	Sr(2)−O(4) × 2	2.768(4)
bond valence sum	2.01	bond valence sum	
Nb(1)−O(2) × 2	1.903(4)	Ta(1)−O(1) × 2	1.911(6)
Nb(1)−O(4) × 2	2.011(4)	Ta(1)−O(2)	1.846(9)
Nb(1)−O(5)	1.877(8)	Ta(1)−O(3) × 2	2.005(6)
bond valence sum	4.841	bond valence sum	5.017
Nb(2)−O(1) × 4	2.006(3)	Ta(2)−O(4) × 2	2.003(6)
Nb(2)−O(1) × 2	1.993(4)	Ta(2)−O(5) × 4	2.009(4)
bond valence sum	4.87	bond valence sum	4.898
Li(1)−O(1) × 2	2.193(8)	Li(1)−O(1)	2.096(18)
Li(1)−O(2)	2.102(13)	Li(1)−O(4) × 2	2.097(13)
Li(1)−O(3) × 2	2.117(9)	Li(1)−O(5) × 2	2.210(12)
bond valence sum	0.872	bond valence sum	0.886
Li(2)−O(1) × 2	2.045(10)	Li(2)−O(3) × 2	2.020(13)
Li(2)−O(4) × 2	2.010(8)	Li(2)−O(5) × 2	2.057(16)
bond valence sum	0.954	bond valence sum	0.926
Li(3)−O(1) × 2	1.944(8)	Li(3)−O(1)	2.060(14)
Li(3)−O(2)	2.035(12)	Li(3)−O(2)	1.782(17)
Li(3)−O(5)	1.83(12)	Li(3)−O(5) × 2	1.989(11)
bond valence sum	1.239	bond valence sum	1.211

method using the Shimadzu software. Photoluminescence spectra were recorded on a Fluorat-02-Panorama UV−vis spectrofluorimeter at room temperature. Semiempirical PM6 calculations were performed using MOPAC2007,[29] with periodic boundary conditions and geometries obtained from the single-crystal X-ray diffraction data of $Sr_3Li_6M_2O_{11}$ ($M = Nb^{5+}$, Ta^{5+}).

Results and Discussion

Crystal Growth of $Sr_3Li_6M_2O_{11}$ ($M = Nb^{5+}$, Ta^{5+}). Pale green crystals of $Sr_3Li_6M_2O_{11}$ ($M = Nb^{5+}$, Ta^{5+}) were grown from a reactive $Sr(OH)_2$/$LiOH\cdot H_2O$/KOH flux. In the crystal growth process, KOH acts as a mineralizer and facilitates the formation of $Sr_3Li_6M_2O_{11}$ ($M = Nb^{5+}$, Ta^{5+}). In the absence of KOH and under otherwise identical crystal growth conditions, the reaction mixtures yield crystals of Li_7MO_6 (M = Nb, Ta) rather than of $Sr_3Li_6M_2O_{11}$ (M = Nb, Ta). The crystal growth process is also quite sensitive to the water content of the flux. Reactions performed using essentially anhydrous starting materials do not yield the desired products, while reactions carried out using the hydrated starting materials do result in the desired products. $Sr_3Li_6Nb_2O_{11}$ was obtained as a pure phase, while minor amounts of a 2H- perovskite-related phase (Sr_3LiTaO_6) always cocrystallized in the case of $Sr_3Li_6Ta_2O_{11}$.

Crystal Structures of $Sr_3Li_6M_2O_{11}$ ($M = Nb^{5+}$, Ta^{5+}). $Sr_3Li_6M_2O_{11}$ ($M = Nb^{5+}$, Ta^{5+}) are iso-structural and crystallize in a new structure type in the orthorhombic space group *Pmma*, with unit cell parameters of $a = 10.5834(15)$ Å, $b = 8.3103(13)$ Å, $c = 5.8277(8)$ Å, $V = 512.55(13)$ Å^3, and $Z = 2$ for $Sr_3Li_6Nb_2O_{11}$ and $a = 10.5936(6)$ Å, $b = 8.3452(5)$ Å, $c = 5.8271(4)$ Å, $V = 515.15(6)$ Å^3, and $Z = 2$ for $Sr_3Li_6Ta_2O_{11}$. The crystal structure of $Sr_3Li_6M_2O_{11}$ (M = Nb^{5+}, Ta^{5+}) (Figure 1) contains sheets of interconnected SrO_8 polyhedra that are separated by M−O layers and an intervening LiO_x polyhedral framework. The SrO_8 polyhedral sheets (Figure 2a) consist of infinite chains of $Sr(2)O_8$ containing polyhedra that share edges in the y direction and corners in the x direction; $Sr(1)O_8$ polyhedra further interconnect these chains via face-sharing interactions. The M−O layers located between the Sr−O sheets (Figure 2a) consist of alternating MO_6 octahedra and distorted MO_5 trigonal bipyramids (Figure 2b). The MO_6 octahedra act as linkers between the Sr−O sheets, while the MO_5 trigonal bipyramids connect to one sheet only, with the apex oriented into the interlayer space where it connects to the Li−O framework. The occurrence of Nb^{5+}/Ta^{5+} in a five-coordinate environment is less common, although it has been reported in oxides such as $Na(V_{3-x}Nb_x)Nb_6O_{14}$,[30] $CsUNbO_6$,[31] and KLi_4NbO_5.[32] Nonetheless, the $Sr_3Li_6M_2O_{11}$ (M = Nb^{5+}, Ta^{5+}) oxides

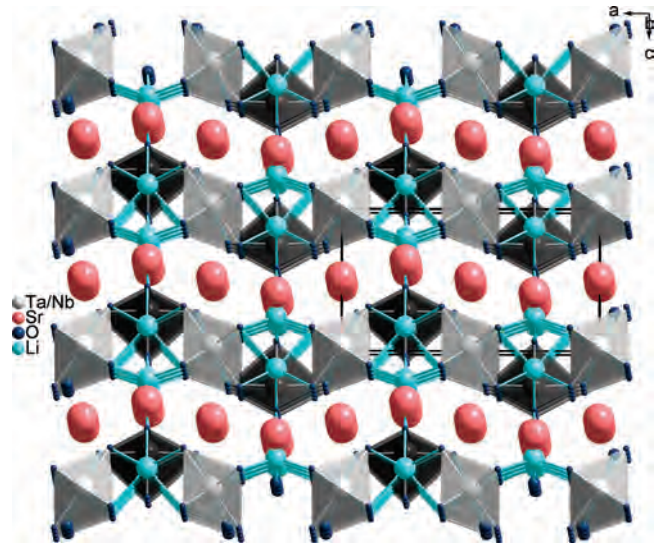

Figure 1. Crystal structure of $Sr_3Li_6M_2O_{11}$ (M = Nb, Ta) oriented along the b axis. MO_5 trigonal bipyramids and MO_6 octahedra are shown as dark and light gray polyhedra, respectively.

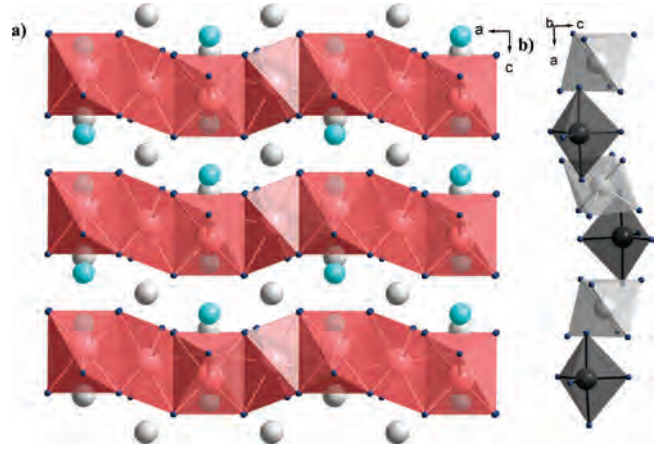

Figure 2. (a) Crystal structure of $Sr_3Li_6M_2O_{11}$ (M = Nb, Ta) shown along the b axis to illustrate the Sr−O sheets. (b) A view of the isolated MO_6 octahedra (light gray) and MO_5 trigonal bipyramids (dark gray).

(29) James Stewart, J. P. *MOPAC 2007*, version 7.101L; Stewart Computational Chemistry: Colorado Springs, CO, 2007.

(30) Koehler, J.; Miller, G.; Simon, A. *Z. Anorg. Allg. Chem.* **1989**, *568*, 8.
(31) Gasperin, M. *Acta Crystallogr.* **1987**, *C43*, 404.
(32) Wehrum, G.; Hoppe, R. *Z. Anorg. Allg. Chem.* **1993**, *619*, 149.

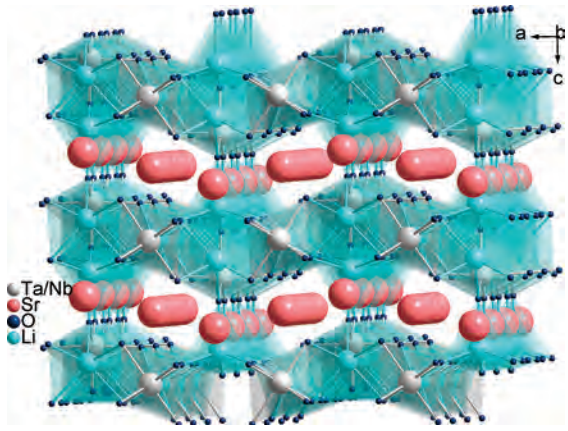

Figure 3. An alternate representation of the crystal structure showing channels formed by NbO_x and LiO_x polyhedra.

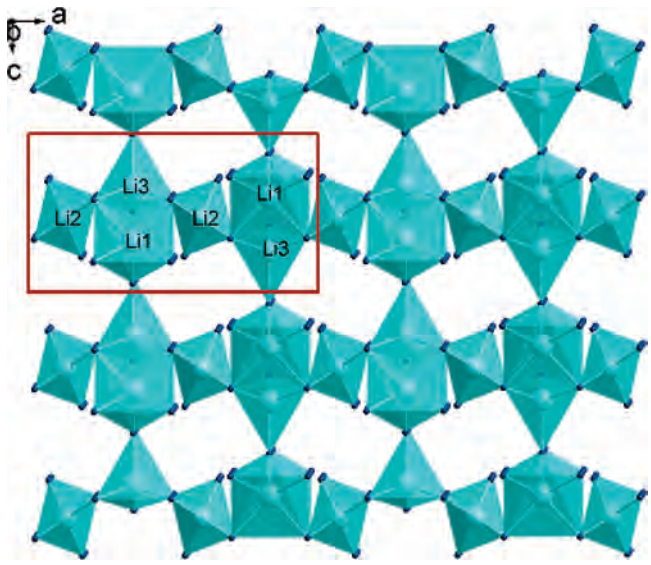

Figure 4. An illustration of the Li−O polyhedral framework in $Sr_3Li_6M_2O_{11}$ (M = Nb, Ta). The repeating unit (brown box) consists of distorted Li(1)O_5 square pyramids and Li(2)O_4 and Li(3)O_4 tetrahedra.

exhibit the rare occurrence of both five- and six-coordinate Nb/Ta in the same structure (Figure 2b), matched by only a few other reported oxides including $A_{1-x}UNbO_{6-x/2}$ ($x = 0$, A = Li, Na, K, Cs and $x = 0.5$, A = Rb, Cs),[33] $Ba_2Nb_{5-x}Ti_xO_9$ ($0 \le x \le 1.75$)[34] and $Rb_4Nb_6O_{17}$.[35] Alternately, the structure can also be described as containing channels formed by NbO_x and LiO_x polyhedra with Sr(1) atoms located in the channels along the a axis and Sr(2) along the b axis (Figure 3).

The presence of lithium in the crystal structure was further confirmed by ^{7}Li NMR measurements (Figures S1 and S2, Supporting Information). The LiO_x polyhedral framework in the crystal structure (Figure 4) consists of distorted Li(1)O_5 square pyramids and Li(2)O_4 and Li(3)O_4 tetrahedra. The framework along the b axis consists of repeating (represented by the brown box in Figure 4) pairs of Li(2)O_4 tetrahedra

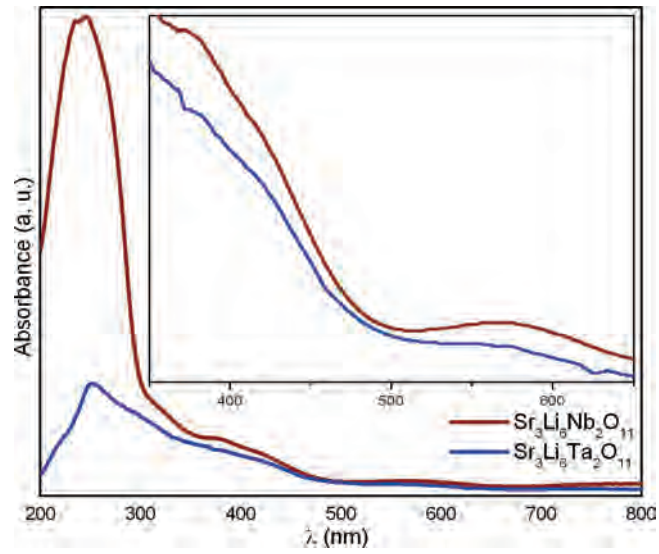

Figure 5. UV−visible absorbance spectra of $Sr_3Li_6Nb_2O_{11}$ (brown) and $Sr_3Li_6Ta_2O_{11}$ (blue) in the range 200−800 nm. Inset shows the presence of color centers in the visible region (350−650 nm).

connected to each other by Li(1)O_5 square pyramids and Li(3)O_4 tetrahedra. Pairs of distorted Li(1)O_5 square pyramids and Li(2)O_4 tetrahedra are edge-shared, while Li(3)O_4 tetrahedra are corner-shared with each other.

The M−O bond distances in $Sr_3Li_6M_2O_{11}$ fall into the range of 1.877(8)−2.011(4) Å and 1.846(9)−2.009(4) Å for M = Nb and Ta, respectively. The apical bond distances in the NbO_5 and TaO_5 trigonal bipyramids are relatively longer (2.011(4) and 2.005(6) Å) than the equatorial bond distances (1.846−1.911(6) Å). The Sr−O bond distances in $Sr_3Li_6Nb_2O_{11}$ and $Sr_3Li_6Ta_2O_{11}$ range between 2.474(4) and 2.749(2) Å and 2.457(6) and 2.768(4) Å, respectively, and are typical for Sr−O bond lengths. The Li−O bond distances in $Sr_3Li_6Nb_2O_{11}$ ((1.830(12)−2.193(8) Å)) and $Sr_3Li_6Ta_2O_{11}$ ((1.782(17)−2.210(12) Å)) are consistent with the reported values for other lithium-containing oxides.[32]

UV−Visible Spectra and Photoluminescence. The UV−visible absorbance spectra illustrate the absorption edges at 285 and 260 nm (corresponding to band gaps of 4.35 and 4.76 eV) respectively for $Sr_3Li_6Nb_2O_{11}$ and $Sr_3Li_6Ta_2O_{11}$, as well as the presence of a shoulder around ~393 nm (Figure 5). A closer examination of the spectra indicates another peak with a λ_{max} of ~560 nm (inset to Figure 5). The presence of two peaks in the visible region (λ_{max} values of ~393 nm and ~660 nm) are typical of color centers[36] in oxides formed during crystal growth by the trapping of electrons or holes at different types of point defects. It is not uncommon that during the flux synthesis of crystals the formation of point defects that act as color centers is facilitated.[37,38]

$Sr_3Li_6Nb_2O_{11}$ and $Sr_3Li_6Ta_2O_{11}$ exhibit violet luminescence upon excitation at 250 nm under a hand-held UV lamp.

(33) Surble, S.; Obbade, S.; Saad, S.; Yagoubi, S.; Dion, C.; Abraham, F. *J. Solid State Chem.* **2006**, *179*, 3238.
(34) Svensson, G.; Eriksson, L.; Olofsson, C.; Holm, W. *J. Alloys Compd.* **1997**, *248*, 33.
(35) Serafin, M; Hoppe, R. *Rev. Chim. Miner.* **1983**, *20*, 214.
(36) Hersh, H. N. *J. Electrochem. Soc.* **1971**, *118*, 44C.
(37) Aleksandrovsky, A. S.; Arkhipkin, V. G.; Bezmaternykh, L. N.; Gudim, I. A.; Krylov, A. S.; Vagizov, F.; Kirensky, L. V. *J. Appl. Phys.* **2008**, *103*, 083102–1.
(38) Ilangovan, R.; Balakumar, S.; Subramanian, C. *Mater. Sci. Technol.* **1999**, *15*, 132.

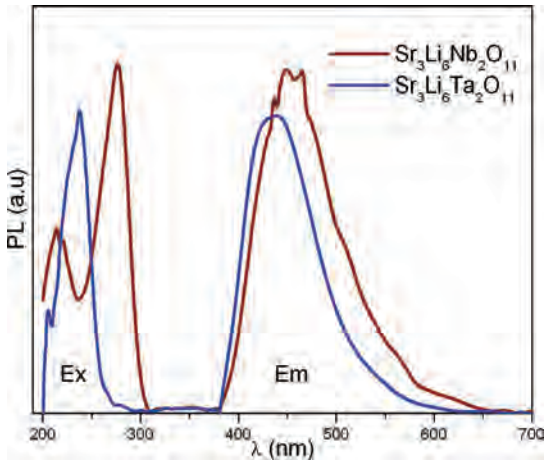

Figure 6. Photoluminescence spectra of $Sr_3Li_6Nb_2O_{11}$ (brown) and $Sr_3Li_6Ta_2O_{11}$ (blue). The excitation (Ex) and emission (Em) peaks are shown on the left- and right-hand sides of the plot, respectively.

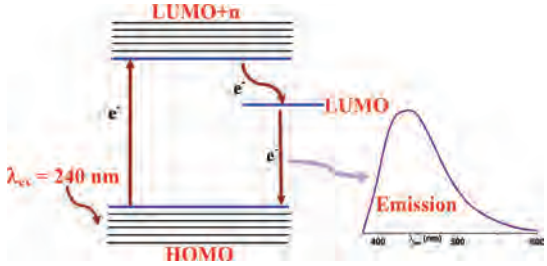

Figure 7. A schematic representation of the likely process of photoluminescence in $Sr_3Li_6M_2O_{11}$ (M = Nb, Ta).

Figure 6 shows the detailed excitation and emission spectra. Maximum intensities in the emission spectra were obtained when using excitation wavelengths of 277 and 238 nm for $Sr_3Li_6Nb_2O_{11}$ and $Sr_3Li_6Ta_2O_{11}$, respectively. Peak shapes in the emission spectra were observed to be broad with wavelength maxima at 448 and 437 nm for $Sr_3Li_6Nb_2O_{11}$ and $Sr_3Li_6Ta_2O_{11}$, respectively, corresponding to violet emission. Attempts to heat the samples at higher temperatures to "anneal" the structure and to remove point defects and color centers were unsuccessful and instead resulted in structural phase transitions, thus limiting our ability to investigate the effect of temperature on photoluminescence.

Photoluminescence in self-activated, non-lanthanide oxides often arises due to the delocalization of electrons in various defect levels or energy states lying within the band gap of the materials.[39,40] Green luminescence in perovskites, such as $BaTiO_3$ and $KNbO_3$, has been attributed to charge-transfer vibronic excitons, specifically, the radiative recombination of self-trapped electrons and hole polarons, on the basis of semiempirical calculations using the Hartree−Fock formalism.[40] Our earlier studies[20] on the mechanism of photoluminescence in Sr_3NaMO_6 (M = Nb, Ta) revealed the existence of an energetically localized excited state, apparently capable of trapping excited electrons and thereby preventing radiation-less decay. A similar approach was followed in our investigation of the electronic distribution of the excited state in $Sr_3Li_6Nb_2O_{11}$ and $Sr_3Li_6Ta_2O_{11}$. Computation of the wave function of $Sr_3Li_6Nb_2O_{11}$ using the MOPAC2007[29] package, unfortunately, did not lead to convergence. However, convergence was achieved upon using a non-default algorithm,[41] yielding a wave function with a large highest occupied molecular orbital−lowest unoccupied molecular orbital (HOMO−LUMO) gap (~7.5 eV) and no energetically localized LUMO.

Convergence difficulties are sometimes associated with wave function degeneracies due to strain in the computed geometries, and therefore, we attempted to minimize the crystal structure of $Sr_3Li_6Nb_2O_{11}$ within the PM6 model. The relaxation lowered the energy by 27.6 eV/unit cell and did yield the energetically localized LUMO orbital, but the optimized crystal structure was different from the experimental one. It is likely that the PM6 model is not suitable for detailed structural investigations of complex inorganic oxides. Density functional theory calculations on these compounds are beyond our current computational capabilities.

A scheme of the potential process of photoluminescence in these oxides is shown in Figure 7. Upon excitation, an electron is promoted from the valence band or HOMO (comprised of O 2p orbitals) to the conduction band or LUMO. From these LUMO+n excited states, there is a nonradiative transfer to an intermediate low-lying LUMO state. In this LUMO state, the electrons are delocalized and do not easily migrate to nonradiative quenching sites, resulting in a subsequent de-excitation to the ground state with violet emission. It is possible that an excitonic mechanism, similar to the one reported for perovskite-type oxides,[40] is responsible for the luminescence in the oxides reported in this paper.

Conclusion

Pale green crystals of $Sr_3Li_6M_2O_{11}$ (M = Nb^{5+}, Ta^{5+}) were grown out of molten hydroxide fluxes. The oxides crystallize into a new structural type consisting of sheets of interconnected SrO_8 polyhedra that are separated by M−O layers and an intervening LiO_x polyhedral framework. These oxides represent one of the few examples where niobium and tantalum exhibit both 5-fold and 6-fold coordination environments in the same structure. Both oxides exhibit violet emission at room temperature upon excitation at a wavelength of 250 nm.

Acknowledgment. Financial support from the National Science Foundation through Grants DMR:0450103 and DMR: 0804209 is gratefully acknowledged. We thank Prof. Shiou-Jyh Hwu, Clemson University, for access to the UV−visible spectrophotometer.

Supporting Information Available: Additional spectra, and CIFs are available. This material is available free of charge via the Internet at http://pubs.acs.org. Further details of the crystal structure investigations can be obtained from the Fachinformationszentrum Karlsruhe, 76344 Eggenstein-Leopoldshafen, Germany (fax: (49) 7247-808-666; e-mail: crystdata@fiz-karlsruhe.de) on quoting the depository numbers CSD-418987 and 418988.

IC801102T

(39) Vikhnin, V. S.; Eglitis, R. I.; Kapphan, S. E.; Borstel, G.; Kotomin, E. A. *Phys. Rev.* **2002**, *B65*, 104304.
(40) Eglitis, R. I.; Trepakov, V. A.; Kapphan, S. E.; Borstel, G. *Solid State Commun.* **2003**, *126*, 301.
(41) Camp, R. N.; King, H. F. *J. Chem. Phys.* **1981**, *75*, 268.